In the IP of the Beholder: Strategies for Active IPv6 Topology Discovery

Robert Beverly
Naval Postgraduate School
rbeverly@nps.edu

Ramakrishnan Durairajan
University of Oregon
ram@cs.uoregon.edu

David Plonka
Akamai Technologies
plonka@akamai.com

Justin P. Rohrer
Naval Postgraduate School
jprohrer@nps.edu

ABSTRACT

Existing methods for active topology discovery within the IPv6 Internet largely mirror those of IPv4. In light of the large and sparsely populated address space, in conjunction with aggressive ICMPv6 rate limiting by routers, this work develops a different approach to Internet-wide IPv6 topology mapping. We adopt randomized probing techniques in order to distribute probing load, minimize the effects of rate limiting, and probe at higher rates. Second, we extensively analyze the efficiency and efficacy of various IPv6 hitlists and target generation methods when used for topology discovery, and synthesize new target lists based on our empirical results to provide both breadth (coverage across networks) and depth (to find potential subnetting). Employing our probing strategy, we discover more than 1.3M IPv6 router interfaces from a single vantage point – an order of magnitude more than produced by current state-of-the-art mapping systems that use hundreds of vantages. Finally, we publicly share our prober implementation, synthesized target lists, and discovered IPv6 topology results.

1. INTRODUCTION

As of May 2018, about 23% of Google's users access their services via IPv6 [21], while APNIC reports that ∼15k Autonomous Systems (ASes) advertise IPv6 prefixes [24]. The number of IPv6 routes in the BGP system has increased from ∼5k in 2011 to more than 48k today [24], while native IPv6 adoption and traffic continues its exponential increase [10]. Similarly, a large content delivery network (CDN) observed 1.72B unique native IPv6 addresses for 576 million unique `/64` prefixes on March 17, 2018 [37]. In a weeks' time, the number of IPv6 `/64`s covering active WWW clients approximated the total number of globally routed IPv4 unicast addresses (∼2.5B). These examples suggest that IPv6 adoption is *here*, underscoring the acute need for accurate IPv6 topologies within the community.

Understanding the Internet's IPv6 topology is important for applications ranging from improved content distribution and traffic optimization, to better address anonymization [36] and reputation [8, 26], to enhanced network security [46, 44]. Despite these compelling applications, three challenges remain: *(i)* an infeasibly large address space that cannot be exhaustively scanned or uniformly sampled effectively, *(ii)* mandated and aggressive ICMPv6 rate limiting in routers [9], and *(iii)* unknown address allocation policies and subnet structures. Note that the first two issues are inter-related: attempting to increase coverage by probing more of the IPv6 address space necessitates faster probing rates. However, increasing the probing rate is self-defeating as doing so triggers more rate limiting and, hence, fewer discovered router interfaces and less accurate topologies.

While decades of research have developed and refined active IPv4 topology discovery [43, 25], these techniques do not address the aforementioned challenges unique to IPv6. Existing IPv6 topology mapping systems are thus forced to directly apply IPv4 discovery tools and techniques. For example, production CAIDA and RIPE Atlas traceroutes regularly, probe the `::1` address of every global IPv6 BGP prefix [7]. Because of this very sparse sampling, the completeness and quality of the resulting logical topologies are unknown.

In this work, we seek to advance the state-of-the-art in Internet-wide IPv6 active topology mapping. Our methodology tackles two fundamental aspects of the problem: which addresses to target and how to probe.

First, we amass *the* largest collection of IPv6 target addresses/seeds from a variety of sources (e.g. BGP, DNS, CDNs [16, 38, 41, 18]) as well as generated seeds (e.g. 6Gen [34]). We employ a three-step process to synthesize 12.4M target addresses. Next, we perform 45.8M traces, in total, from three vantages: two US universities and one EU network. We investigate different target selection methods and parameters (e.g. maximum TTL, protocol, probing speed, etc.) to elicit the most IPv6 topological information. We show that our methodology provides breadth across networks, depth to discover subnetting, and speed. Employing our probing strategy, we discover >1.3M IPv6 router interfaces from a single

vantage in a single day – an order of magnitude more than produced by current state-of-the-art mapping systems that use hundreds of vantages in the same period. Our primary contributions thus include:

- Evaluation of various means to synthesize target addresses from seven different input seeds.
- Quantification of random probing to maintain high rates while avoiding ICMPv6 rate limiting.
- Extensive characterization of target list power and the resulting topologies.
- IPv6 subnet discovery as a case study of topological inference.
- Public IPv6 topology maps, our synthesized target lists, and our prober implementation [5].

2. BACKGROUND AND RELATED WORK

IPv6 topology. Dhamdhere et al. studied the evolution of IPv6 topology at the AS level using passive BGP data and found that fewer than 50% of AS-level paths in 2012 were identical between IPv4 and IPv6, while a single AS (Hurricane Electric) was dominant in the topology [13]. Similarly, Czyz et al. examined BGP tables in 2013 and, while they found only 19% of ASes supporting IPv6 as compared to IPv4, a k-core analysis showed that these ASes were well-connected large networks with high centrality [10]. Complementary to these efforts, we take an in-depth look at the IPv6 topology, starting from an interface-level perspective, after a period of sustained growth, via *active* probing.

Prior IPv6 topology work has largely avoided active probing due to the sheer size of the address space and the sparsity of infrastructure within it. Presently, two production measurement platforms continually perform active IPv6 topology mapping: CAIDA's Ark [7] and RIPE Atlas [39]. These systems send paris traceroute probes toward the `::1` address in each IPv6 prefix present in the global BGP table. A central finding of our work is that using BGP prefixes to guide target selection works well to capture topological breadth, but not depth, i.e. it does not discover subnetting.

Rohrer et al. uniformly sampled the IPv6 Internet by tracerouting to an address in each routed /48 prefix [40]. Their study issued ten times as many traces as our work, yet found an order of magnitude fewer interfaces – again demonstrating the necessity to perform finer-grained probing within some prefixes to discover extant subnetting and the routers supporting the subnets.

More broadly, prior studies of IPv6 topology use traditional tools including `traceroute6` [32] and `scamper` [29]. Gaston was the first to explore higher-rate IPv6 active topology probing [19] via randomization, and demonstrated the ability to capture roughly an equivalent amount of topological information as collected via CAIDA's Ark system. However, Gaston's study did not examine the critical problem of target selection and rate-limiting, and did not explore the ability to utilize high-speed probing to discover a larger swath of the topology. Alvarez et al. developed and evaluated methods to deal with ICMPv6 rate-limiting problems, but in a stateful, proprietary prober [2].

Figure 1: IPv6 topology target generation: addresses from various *seeds* are transformed into *intermediate prefixes* which are then synthesized into *targets*.

IPv6 hitlists. Cataloging active IPv6 addresses in the Internet, commonly known as a *hitlist*, has been of interest to the measurement community over the last decade. Notable efforts leverage active (e.g. random probing of `::1` [7], exhaustive probing of one address in each `/48` in all advertised `/32`s [40], and recursive querying of DNS [16]) and passive techniques (e.g. from BGP updates [13, 24], traffic captures [12]) as well as a number of passive and active sources [18]. We provide details of the specific hitlists we utilize in §3.1.

IPv6 addresses/deployments. Many issues pertinent to our work – including seed sources, target selection, and probing techniques – reflect current understanding of IPv6 network reconnsaissance [20]. Malone analyzes different aspects of three IPv6 address datasets and presents an analysis technique to learn about their deployments and usages [32]. Czyz et al. [11] studied 520k and 25k dual-stacked servers and routers and compared the security policies of IPv4 and IPv6 deployments. To assess the lifetime and density of billions of IPv6 addresses, Plonka & Berger developed Multi-Resolution Aggregate plots and classified addresses spatially and temporally [35]. A recursive algorithm to discover and extract IPv6 addressing patterns is discussed in [45]. Similarly, Foremski et al. proposed a system called Entropy/IP to uncover the structure of IPv6 addresses using machine learning [17]. In a similar vein, Murdock et al. designed "6gen" target generation [34]. 6Gen exploits address locality: discovery of new targets happens closer to highly dense ranges. In a nybble, targets are generated either based on a specific range (e.g. `2::[1-4]:0`) or wildcard (e.g. `2::?:0`); the former is *tight* clustering while the latter is referred as *loose*.

3. TARGET SELECTION

Our methodology tackles two primary challenges: *(i)* selecting targets from the large and sparsely populated IPv6 address space; and *(ii)* effectively sourcing probes. We consider the first challenge in this section.

3.1 Target Generation

We employ a three step process, outlined in Figure 1,

Table 1: Seed List Properties

Name	Method	Date yyyy-mm-dd	# Addrs	Interface Identifiers					
				Random		LowByte		EUI-64	
CAIDA [7]	BGP-derived	2018-05-09	105.2k	53.7k	51.02%	51.5k	48.98%	0	0.00%
DNSDB [41]	Passive DNS	2018-04-28	5.4M	1.3M	24.43%	2.2M	41.27%	146.5k	2.74%
Fiebig [16]	Reverse DNS	2018-03-27	11.7M	4.2M	35.94%	3.2M	27.54%	275.4k	2.35%
FDNS [38]	Fwd. DNS	2018-04-27	24.8M	3.3M	13.12%	7.0M	28.20%	236.8k	0.95%
CDN Clients [36]	*k*256 Agg.	2018-03-03	N/A	All	100.00%	0	0.00%	0	0.00%
	*k*32 Agg.	2018-03-03	N/A	All	100.00%	0	0.00%	0	0.00%
6gen [34]	Generative	2018-02-13	4.9M	4.4M	89.61%	389.2k	7.93%	17.1k	0.35%
Combined	Join Sets	Varies	50.8M	13.2M	28.19%	12.9M	27.45%	675.8k	1.44%
TUM [18]	Collection	Varies	5.6M	2.3M	44.62%	1.2M	23.54%	604.0k	11.79%
Random	Random	2018-05-23	26.5M	0	0.0%	95.8k	0.36%	0	0.0%

to prepare a set of *targets*, based on a set of *intermediate prefixes*, which are synthesized from *seeds*. The targets are IP addresses to be used as destinations for TTL-limited probes emitted from a *vantage*.

Step 1: Seed Sourcing. A list of *seeds* is obtained from a *source*. Our seeds are either IP prefixes (base address and length) or IPv6 addresses (base address with implicit 128b length), which are used as hints to select interesting areas of the address space that bound probe destinations.

Step 2: Prefix Transformation. One or more *transformations* may be applied to the seeds to yield a set of *intermediate prefixes*. Depending on the transformation method, the resulting set might have the same or fewer number of prefixes than the seed list to which it was applied. The prefix transformations used in this study are as follows:

- **k*n***: Perform kIP aggregation-based address anomymization with parameters: $w = 14$ (window days), $i = 1$ (interval hours), $k = n$ (simultaneously-assigned /64 prefixes), $p = 50$ (50th percentile of intervals). [36], *e.g.,* **k32** and **k256**.
- **z*n***: Extend input prefixes with length $< n$ to /n, i.e. base address set to zeroes after the nth bit; aggregate input prefixes having length $> n$ to /n prefixes.

Step 3: Target Synthesis. Lastly, a *synthesis* method takes the intermediate prefixes as input and yields a set of target addresses. The target synthesis methods used in this study are as follows:

- **lowbyte1**: bitwise OR prefix base address with IID value `:0000:0000:0000:0001`.
- **fixediid**: bitwise OR prefix base address with IID value `:1234:5678:1234:5678`.

With each method, we remove any duplicate target address within each set. The target address sets are now ready to be employed in a probe *campaign*.

3.2 Seeds

The seed sources used in this study are as follows:

- **caida**: The set of probe targets selected by CAIDA, based on BGP-advertised IPv6 prefixes of size /48 or larger, i.e. prefixes with length of at most 48 bits [7].
- **fiebig**: The set of IPv6 addresses gleaned from walking the `ip6.arpa` zones in the DNS [16].
- **fdns_any**: A set of IPv6 addresses found in DNS answers in response to forward DNS ANY queries performed by Rapid7's Project Sonar.[38].
- **dnsdb**: A set of IPv6 addresses found in DNS answers passively observed in AAAA DNS query responses by Farsight Security's Farsight Passive DNS project and anonymized and imported into Farsight DNSDB [41]. We queried DNSDB all IPv6 records observed between 15 Feb and 28 Apr 2018 in the covering set of all advertised BGP IPv6 prefixes (as reported by RouteViews [1] on 20 Apr 2018).
- **cdn**: A set of IPv6/64 prefixes that covered the set IPv6 WWW client addresses thought to be SLAAC temporary privacy addresses, as observed by a large Content Delivery Network (CDN) across 14 days, February 18, 2018 through March 3, 2018 (UTC). [1]
- **6gen**: A set of IPv6 address synthesized using 6Gen tool in loose clustering mode [34]. The input to the tool is a combination of IPv6 destinations probed and new interfaces found from probing those destinations by CAIDA on March 06, 2018.
- **tum**: A combined set of IPv6 addresses created by combining multiple existing address sets including some that we also use individually (fdns_any) and a number of others (openipmap, ct, caida-dnsnames, alexa-country, traceroute, and traceoute-v6-builtin). Some of these subsets are documented in [18] and others are undocumented. Each subset is packaged separately, and we noted some anomalies (such as zero-size of very small files for recent dates) leaving room for interpretation as to what would best represent the TUM dataset as a whole. With this in mind we took the most recent and largest file for each subset, which are shown in Table 2.

We examine several features of our seed lists in Table 1. At a glance we note the wide variance in size (105k addresses to 25M). The seeds are derived using widely varying methodology, which we hope makes them

[1]The authors were only provided these anonymous aggregate covering prefixes of the clients rather than live user addresses.

Table 2: TUM Subsets

Filename	Addrs
alexa-country-2018-04-23.csv	1,634
caida-dnsnames-2018-01-17.csv	1,268,982
caida-dnsnames-2018-04-25.csv	16,507
ct-2018-04-27.csv	21,983,387
openipmap-2018-04-23.txt	11,149
rapid7-dnsany-2018-03-30.csv	24,959,477
rapid7-dnsany-2018-03-31.csv	14,434,117
traceroute-2018-04-24.txt	128,398
traceroute-v6-builtin-2018-02-25.txt	112,754
All zone files from 2018-04-27	17,173,243
Total	80,089,648
Total Unique	**5,599,313**

complementary (not redundant). We specify the date of acquisition; in cases where the seeds correspond to a range of dates, just the end date is specified in the table to conserve space. The full range is given in Step 1. In addition we perform of rough classification of the IIDs in order to inform our choice of target IID, as well as enable correlation with result sets.

We classified our seed addresses using the `addr6` tool [42]. This tool examines each address, looking for patterns, such as whether the IID, *e.g.*, *(i)* may be an EUI-64 IID with an embedded MAC address ("IEEE-based"), *(ii)* has a run of zeroes followed only by a low number ("lowbyte"), or *(iii)* has no discernible pattern ("randomized", essentially meaning unrecognized).

A few notes on particular seed lists are worth mentioning. The CDN Clients individual IPv6 addresses are unavailable to the authors due to privacy concerns, instead prefixes are provided, generated using the kIP aggregation approach described in §3.1. While the number of addresses aggregated is unknown, we received 421,807 aggregates in the CDN-k256 set and 3,445,329 aggregates in the CDN-k32 set. We treat the first 6 seed lists in Table 1 as independent. We create our own combined list by joining those 6 lists. The TUM list is also a collection [18], which includes CAIDA and FDNS subsets, and therefore is not independent of the first 6 lists. Lastly, we randomly generate 26.5M targets in BGP routed IPv6 address space as a control seed list.

3.3 Selecting Transformations

Prefix transformation granularity. Next, we seek to understand the influence of aggregation granularity when performing prefix transformation. Many of our seed input datasets contain multiple IPv6 addresses within the same /64 prefix – this is a natural consequence of their intended use as hitlists for IPv6 host discovery, rather than IPv6 router discovery. Intuitively, assuming that /64 prefixes are frequently allocated to customers and represent the smallest IPv6 subnet, we would not expect traceroutes to multiple addresses within the same /64 to yield different topologies.

To characterize the relationship to the discovered topology, and the probing required when using **z*n***, we probed the fDNS_any dataset for varying values of n. Table 3 shows that **z64** requires more than eight times as many probes as **z40**, but discovers three times as many unique interfaces. More importantly, we consider the number of interfaces that are discovered exclusively as a result of using a particular aggregation level. Although **z64** requires significant probing, there are more than 27k interfaces that only discovered using this aggregation level. Finally, we examine the number of non-time exceeded responses from each of the aggregation levels. The number of other-ICMP6 responses per probe is 0.012, 0.029, 0.032, and 0.041 for $n = 40, 48, 56, 64$. Thus, after normalizing to the number of probes, the $n = 64$ aggregation level has the effect of producing a higher rate of non-time exceeded responses, suggesting that these probes are reaching further into the network.

Table 3: Aggregation Level

z*n*	Probes	Other-ICMP6	Ints	Excl Ints
/40	1.4M	17.5k	27.0k	158
/48	3.6M	105.8k	45.5k	321
/56	6.1M	194.8k	60.5k	1.1k
/64	11.8M	486.8k	85.5k	27.2k

Table 4: Host Identifier

type/code	CDN		Fiebig
	lowbyte1	fixediid	known
Hop lim	98.1%	98.1%	95.8%
No route	0.7%	0.7%	0.6%
Adm prohib	0.6%	0.6%	0.4%
Addr unrch	0.3%	0.4%	0.7%
Port unrch	0.1%	0.0%	2.3%
Reject rte	0.1%	0.2%	0.2%

Target synthesis. The lower 64 bits of an IPv6 address denote the interface identifier [23]. Given a candidate prefix, we must select the host identifier within that prefix to probe toward. Natural candidates are the `::1`, a random identifier, a known host identifier from the input seed list, or a fixed pseudo-random identifier. In addition to understanding whether this choice has an impact on topological discovery, we further wish to expose the extent to which different identifiers elicit non-Time-Exceeded messages as a metric of impact on hosts. We therefore mounted a campaign using the cdn-k256 prefixes and both the **lowbyte1** and **fixediid** host identifiers for target synthesis. Table 4 shows the distribution of ICMP6 responses received as a result of the campaigns.

First, we find that more than 98% of responses are ICMP6 time exceeded messages as we expect. We see only negligible differences between **lowbyte1** and **fixediid**; **lowbyte1** produces five times as many ICMP6 port unreachable responses, but the total number of such responses is still very small. To understand the use of a known address within the prefix, we further compare against probes toward known addresses within the Fiebig seed list. In contrast to probing the base or fixed identifier, port unreachable messages constitute 2.3% of the

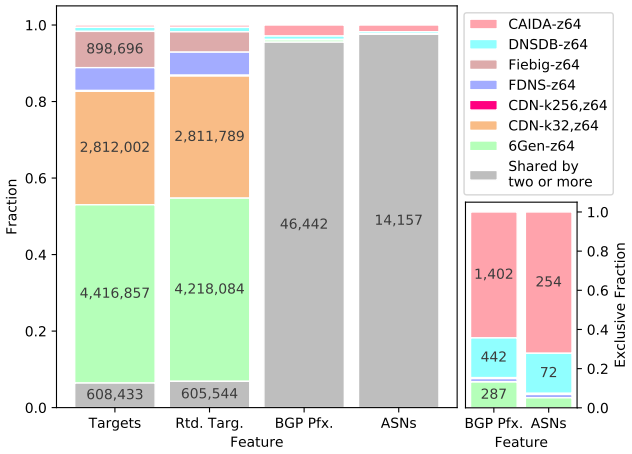

Figure 2: Features contributed by each target set

distribution for the known address probing, suggesting that our probing is reaching these end hosts.

Because we observe only minimal impact on discovery between fixed interface identifiers and the base address, we choose to use the fixed identifier for the remainder of the experiments in order to minimize any potential impact on end hosts.

3.4 Target Set Characterization

After aggregating the seeds into our target sets, we characterize and compare them across multiple dimensions in Table 5. Unique targets refers to the number of targets in the set after duplicates have been removed. Exclusive features are those found only in one of the sets and not any other set. We find that most of the sets have some fraction of targets that are not found in the public BGP IPv6 routing tables, and in some cases (e.g. Fiebig) this fraction is significant, so the "Routed Targets" and "Excl R-Targ" columns characterize only the subset of targets that appear in BGP. Additionally we note that some target sets, despite a large number of targets, are concentrated in only a few BGP prefixes and ASNs, based on the number of BGP prefixes and ASN represented in each set.

As mentioned in §3.1, some seed lists, and consequently the corresponding target sets are not independent of others. When computing features that are exclusive to the first 14 sets listed (CAIDA–6Gen), we do not consider the Combined sets we created, or the TUM sets, since they would cancel out the exclusive contributions of their respective subsets. For the TUM sets, however, we do show the features that are found in that set exclusively. The "Total" sets merely allow us to refer to the total number of unique features that exist across all the sets, those sets are not probed independently.

Figure 2 shows the break-out of features contributed exclusively by each z64 target set. Clearly there are a few large players in terms of number of targets/routed

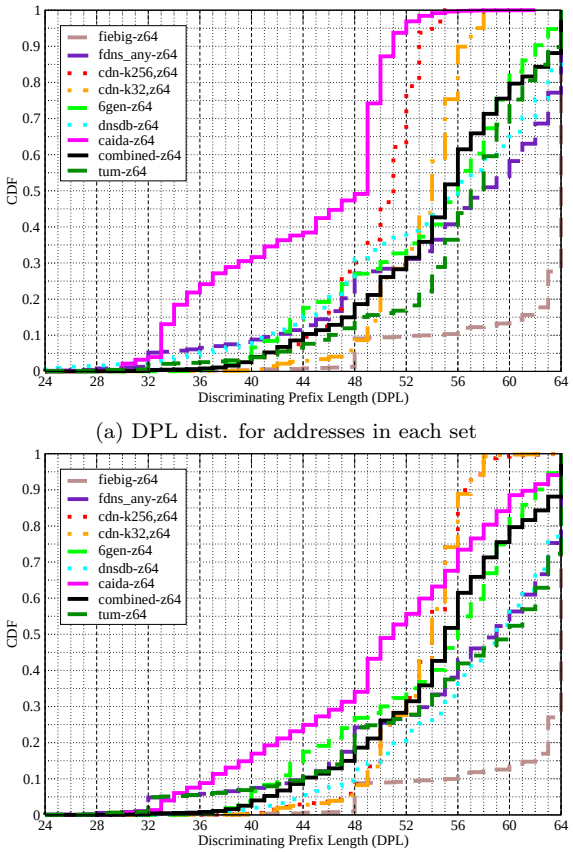

(a) DPL dist. for addresses in each set

(b) DPL dist. when sets are considered together

Figure 3: Discriminating Prefix Length (DPL) Distributions for target sets (CDF)

targets, however this does not strongly correlate to representation in BGP or ASNs. Since the vast majority of BGP prefixes and ASNs are represented in more than one target set, we provide an alternate inset view of those two features with the shared contribution removed. From this we can clearly see the lack of correlation between target set size and those two features.

3.4.1 *Discriminating Power*

In this work we rely heavily on the notion of address' discriminating prefix length (DPL).[2] An address' DPL is the first (leftmost) bit at which it differs from it's nearest address accompanying it in a (sorted) set, e.g. one of our target sets. From left to right (high to low order) bits across the address, the DPL is how far one must compare addresses, bit by bit, to discriminate them from each other, for instance how a primitive router might determine which way to forward traffic if two addresses required different treatment. As such, the DPLs of addresses in a set capture their proximity to each other – the higher the DPLs the closer the addresses are – and,

[2]Kohler et al. [27] introduced the term "discriminating prefix length." It has been employed in the structure analysis of both active and passive measurements.

Table 5: Target Set Properties

Name	Agg	Uniq Targs	Excl Targets	Routed Targets	Excl R-Targ	BGP Prefixes	Excl BGP	ASNs	Excl ASNs	6to4
CAIDA	z48	78.3k	26.4k	76.2k	25.4k	47.5k	1.4k	14.4k	254	0
	z64	105.2k	56.6k	102.7k	55.2k	47.6k	1.4k	14.4k	254	0
DNSDB	z48	93.8k	9.3k	93.3k	9.4k	36.5k	360	12.8k	73	80
	z64	233.0k	101.1k	231.9k	101.0k	36.7k	442	12.8k	72	80
Fiebig	z48	102.2k	85.4k	45.1k	28.8k	6.0k	8	3.9k	2	0
	z64	1.0M	898.7k	576.9k	468.8k	6.0k	11	3.9k	2	0
FDNS	z48	228.7k	171.8k	193.0k	136.7k	13.4k	17	7.7k	5	88.4k
	z64	746.9k	566.3k	709.9k	530.4k	13.5k	34	7.7k	6	88.5k
CDN-k256	z48	162.4k	2.6k	162.3k	2.6k	3.3k	0	589	0	160
	z64	396.7k	19.6k	396.6k	19.5k	3.3k	0	589	0	160
CDN-k32	z48	524.2k	341.8k	523.9k	341.6k	4.9k	3	1.2k	0	1.4k
	z64	3.2M	2.8M	3.2M	2.8M	4.9k	4	1.2k	0	1.4k
6Gen	z48	1.4M	1.4M	1.3M	1.3M	44.3k	171	13.8k	17	0
	z64	4.5M	4.4M	4.3M	4.2M	44.5k	287	13.8k	18	0
Combined	z48	2.3M	N/A	2.1M	N/A	48.3k	N/A	14.5k	N/A	89.9k
	z64	9.5M	N/A	8.8M	N/A	48.6k	N/A	14.5k	N/A	90.0k
TUM	z48	362.7k	108.4k	305.3k	86.0k	25.6k	36	10.9k	10	91.0k
	z64	2.1M	1.3M	2.0M	1.3M	25.9k	158	10.9k	20	91.2k
Total	z48	2.4M	N/A	2.2M	N/A	48.3k	N/A	14.5k	N/A	100.7k
	z64	10.8M	N/A	10.1M	N/A	48.8k	N/A	14.5k	N/A	100.9k
	both	12.4M	N/A	11.5M	N/A	48.8k	N/A	14.5k	N/A	114.9k

when two addresses are topologically heterogeneous, e.g. in different subnets, the addresses' DPL is a lower bound on their respective subnets' prefix length. We will first employ DPL to characterize our target sets. Later, in §6, we will use DPL when discovering network topology from trace results.

Figure 3a explores the potential power of each target set to discriminate addresses and subnets, on its own. Note how the distribution of discriminating prefix lengths characterizes a target set. For instance, about 50% of the `caida-z64` target addresses have a DPL less than 48, i.e. they do not share the same top 48 bits, and therefore are not covered by the same /48 prefix. In contrast, over 70% of the `fiebig-z64` target addresses have DPL of 64, meaning the addresses share the top 63 bits, i.e. are very near one another.

Figure 3b explores the increased potential discriminating power that each target set brings when they are used in combination. For example, the `caida-z64` distribution shifts right, meaning that some addresses from other target sets are interleaved amongst the its target addresses, thus yielding more power to discover routers hops on paths to more (specific) routed prefixes or subnets. One might say addresses in some target sets cleave apart addresses in others, yielding a more powerful combined target set in depth as well as breadth. In contrast, note that the distribution of `fiebig-z64` is unaffected by the combination. This is largely because it has densely-arranged target addresses, 89% of which are unique amongst all target sets (see Table 5).

Note Figure 3b allows us to make *predictions* about the discriminating power of the target sets in combination with each other as measured by a shift rightward to higher DPL values. For instance, `cdn-k256,z64` when combined with `cdn-k32,z64` discriminating power shifts to that of latter, which happens to contain 94% of the targets in the former. Also, combining `fdns_any-z64` with `tum-z64` converge to similar discriminating power. Presumably this is a side-effect of the latter largely including the former. Indeed, 88% of the targets in `fdns_any-z64` are contained in `tum-z64`. Additionally, `dnsdb-z64` roughly converges with `tum-z64` and `fdns_any-z64`, and given that it is also DNS-based, it is plausible to conclude that it explores similar IP-space.

Also noteworthy is what does not change between Figure 3a and Figure 3b. None of the "large" target sets (`cdn-k32,64`; `6gen-z64`; or `tum-z64`) shift noticeably to the right. From this we draw two insights. First, combining significantly smaller sets with large sets has no significant impact on the potential discriminating power of the large set (unsurprisingly), even when significant interleaving occurs. Second, none of our large sets interleave significantly with each other. This is both good and bad, meaning that they are complementary in terms of the regions of IPv6 space explored, with the tradeoff being that they do not reinforce one another to enable addition depth of topology discrimination. If two similarly sized *and* interleaved target sets were combined, we would expect the combined potential discriminating power to be higher than either set individually.

To reiterate, at this stage we are only discussing *potential* discriminating power because these are only target sets; they are not empirically discovered. Yes some target sets are based on addresses of real hosts, but others are synthetically generated.

4. PROBING

We start with Yarrp, a randomized high-speed IPv4

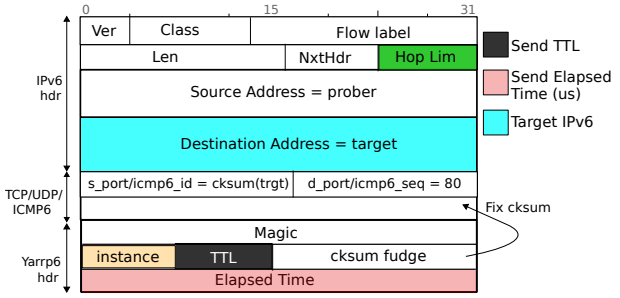

Figure 4: Yarrp6 state: a 12B application payload carries state and corrects the checksum such that the IPv6 and transport headers remain per-target constant.

topology prober [4]. In contrast to traditional traceroute techniques intended to probe individual paths, Yarrp is specifically designed for large-scale Internet-wide topology mapping. Yarrp spreads topology probes across the network rather than probing the path to individual destinations sequentially. It does this by randomly permuting the space of destination targets and TTLs, thereby attempting to avoid overloading any single router or path.

Rather than maintaining large amounts of state as such randomization would impose on a traditional traceroute-based prober, Yarrp encodes details of the probe (e.g. originating TTL and timestamp) *within* the packet so that state can be reconstructed from the ICMP reply. This encoding thus allows Yarrp to be stateless. Yarrp thus decouples probing from topology construction; the complete set of responses to any single destination are not in any order and are intermixed with the responses from all other destinations. Based on promising results measuring IPv4 [4], we explore adapting these techniques to the IPv6 domain.

4.1 Yarrp6

State encoding. IPv6 requires several changes in order to retain the stateless nature of Yarrp. First, IPv6 headers have removed some of the fields used by Yarrp in IPv4 to encode state, e.g. IPID. While there is less room for encoding within the IPv6 packet header, conversely, ICMPv6 affords the advantage of complete packet quotations. Rather than having to encode state into the probe's packet headers such that a partial (28B) packet quotation contains Yarrp state, the ICMPv6 specification requires as much of the packet that induced the TTL exceeded message to be returned as possible [9]. This allows us to encode and recover more state and ensures that header values remain constant so all probes for the same destination follow the same path when load balancing is present [3]. Further, placing state in the payload removes the need to encode data within the transport protocol (for example, IPv4 Yarrp uses the TCP sequence number to encode the timestamp), and thus easily facilitates using multiple transport protocols (Yarrp6 supports TCP, UDP, and ICMPv6).

Figure 4 depicts how Yarrp6 encodes states within the probes it sends. After the IPv4 and transport headers is the Yarrp6 payload of 12B. The Yarrp6 payload consists of a 4B magic number and 1B instance ID to ensures that received ICMPv6 packets are indeed responses to Yarrp6 probes, and for the running instance. A single byte encodes the originating TTL ("hop limit"). Four bytes encode the probe's timestamp to permit round-trip-time (RTT) computation.

We wish to ensure that the packet headers remain constant and accommodate load balanced paths, however the checksum will be different for each probe as the TTL and timestamp in the Yarrp6 payload changes. We therefore include 2B of "fudge" within the Yarrp6 payload in order to ensure that the checksum also remains constant. Finally, we compute a 2B Internet checksum over the IPv6 target address and, depending on the transport protocol selected, use it for the TCP or UDP source port or ICMPv6 identifier. This checksum ensures that the quoted IPv6 target address is unmodified.

Fill Mode. A consequence of stateless operation is that Yarrp cannot stop probing when it reaches its destination, or encounters several unresponsive hops in a row (the so-called "gap-limit") [4]. Instead, the user must select the TTL range to probe a priori, potentially missing hops if the maximum TTL is smaller than the path length, or wasting probes if the maximum TTL is larger than the path length. To better accommodate this tension, we add to Yarrp6 a "fill mode."

Let the user-selected maximum probing TTL be m. In fill mode, if the Yarrp6 listener receives a response for a probe sent with hop limit h where $h \geq m$, it immediately sends a new probe toward the destination with a hop limit of $h + 1$. While these additional probes are not randomized, fills are uncommon and occur at the tail of the path where the effect of sequential probing has the least impact. We explore tuning of Yarrp6 parameters, including fill mode, next.

4.2 Tuning

In addition to selecting vantage points and targets, active topology discovery requires choosing the probing protocol, maximum TTL, speed, and other parameters. This section explores these parameters to better understand the tradeoffs and to guide our probing strategy.

Protocol. Any IPv6 packet can be used for active topology probing, however the well-known prevalence of middleboxes and firewalls suggests that different transport protocols, e.g. TCP SYN, TCP ACK, UDP, or ICMP6, can yield different results depending on whether these are blocked along a path or whether an in-path device maintains connection state. Luckie et al. studied the influence of transport protocol for IPv4 and found that ICMP-paris reaches the most destinations, while UDP based methods infer the greatest number of IP links [31]. CAIDA's production active topology discovery [6, 7]

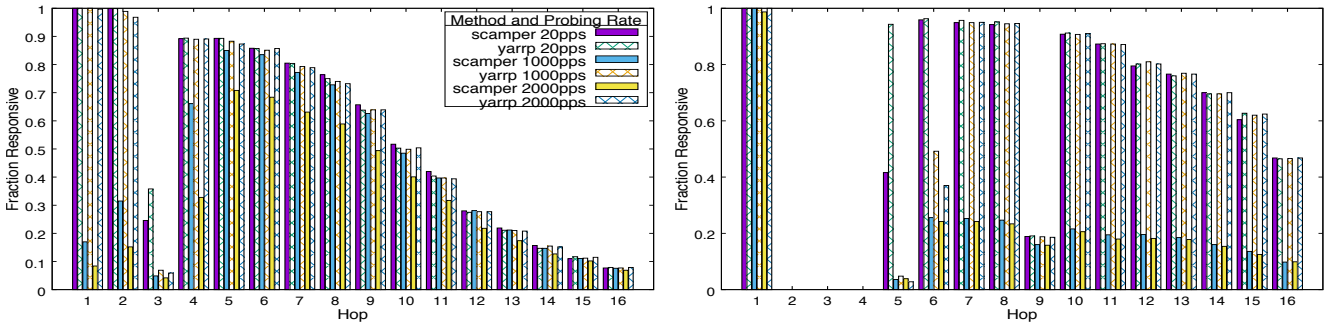

(a) Vantage: US-EDU-3

(b) Vantage: US-EDU-2

Figure 5: Relationship between probing strategy, rate, and per-hop responsiveness at two vantage points. While ICMP6 rate-limiting is clearly evident, randomly permuting the probing order universally improves responsiveness.

utilizes ICMP-paris for both IPv4 and IPv6.

To the best of our knowledge, there is no published equivalent analysis of the effect of transport protocol on IPv6 active topology discovery. We therefore mounted probe campaigns from two of our vantage points on February 1, 2018 using the CAIDA target set. We use the same permutation seed and targets to probe using TCP, UDP, and ICMP6. To mitigate the possible effects of any rate-limiting, we probed at only 20pps.

On average, we see that probing with ICMP6 results in ∼2.2% and 2.1% more discovered interfaces than using UDP and TCP respectively. Interestingly, ICMP6 probes produce on average 13.6% and 24.3% more non-time exceeded ICMP6 responses than UDP and TCP respectively, suggesting that these probes are penetrating deeper into the network. Given these observations, we send ICMPv6 probes for the remaining experiments.

Speed. As discussed previously, probing speed has a potentially greater impact on discovery in IPv6 as compared to IPv4 due to mandated rate-limiting. Toward understanding the behavior of various probing techniques and speeds in production, we mount probing campaigns to the CAIDA target set on April 27, 2018 from our vantage points. Figure 5 shows the fraction of responses received versus the TTL of the probe at speeds of 20, 1000, and 2000 pps. Further, we use both Yarrp6 and scamper [29], the current state-of-the-art topology probing tool. Note that because the number of responsive interfaces decreases as the hop distance increases, it is necessary to compare the relative performance of Yarrp6 and scamper at different speeds.

We observe markedly different results from using scamper versus the permutation of Yarrp6 at speeds above 20pps, especially nearer to the vantage point. For instance, in Figure 5a, while scamper and Yarrp6 have nearly identical response rates at 20pps, Yarrp6 yields a 100% response rate from the first hop for 1000 and 2000pps as compared to less than 20% and 10% for scamper. Across both vantage points, we observe better performance with Yarrp6 at all hops than achieved with scamper at higher probing rates.

Table 6: Fill mode

MaxTTL	Probes	Fills	Interfaces	Yield %
4	375.6k	96.4k	271	0.1
8	751.2k	213.5k	11.3k	1.2
16	1.5M	251.5k	39.1k	2.2
32	3.0M	0	54.1k	1.8

Also of note are the variety of rate-limiting behaviors implemented by routers. For instance, hop 3 of Figure 5a and hops 5 and 9 of Figure 5b appear to implement more aggressive rate limiting as compared to the other hops. Further, while not pictured, we find one hop near one of our vantage points that only responds with time exceeded messages when ICMP6 is used as the probe type. Because subsequent hops respond, we conjecture that this behavior is due to some form of state maintenance for security reasons.

TTL range. As described previously, Yarrp6's fill mode balances the choice of a maximum probe TTL with discovery rate and volume of probing. Recall that the maximum TTL must be selected in advance as part of the permutation process. Thus, a large maximum TTL will potentially waste probes, while a small maximum TTL will potentially miss hops. Fill mode allows us to select a lower maximum TTL, thereby lowering probing volume, while missing fewer hops.

To quantify this tradeoff, we explore the use of different Yarrp6 maximum TTL values when probing the CAIDA target set on May 2, 2018. In all experiments, fill mode continues probing past the maximum TTL so long as responses are received, up to a maximum hop limit of 32. Table 6 shows the number of probes, probes resulting from fills, unique interfaces discovered, and the interface yield (interfaces discovered per probe). Note that a single non-responsive hop past the maximum TTL will cause fill mode to stop. Thus, we observe that the number of fills for a maximum TTL of four is much less than for a maximum TTL of eight simply because hop five did not respond. Using a maximum TTL of 16 produces the highest yield; we therefore use this for the remainder of the experiments in order to achieve the most efficient use of probing.

4.3 Ethical Considerations

Performing large-scale, Internet-wide active measurements requires careful consideration of the experimental methodology to avoid causing harm. First and foremost, we obtained explicit permission from the networks hosting the vantage points in our study. Second, we opt to send ICMPv6 probes as they are relatively innocuous compared to UDP and TCP, are used by the existing Ark and RIPE platforms thereby facilitating direct comparison, and yield the most responses as discussed in §4.2. Third, although capable of much higher rates, we run Yarrp6 at 1kpps both to minimize rate-limiting (§4.2) and to maintain low network load (note that Yarrp's randomization naturally spreads load). Fourth, because our goal is to discover IPv6 router addresses, not end hosts, we use the fixed pseudo-random IID for all campaigns, which is unlikely to be an active IPv6 host. We show in §3.3 that using this IID has neglibible effect on topology discovery as compared to the `::1` IID.

Finally, we follow best practices for good Internet citizenship by making an informative web page, along with opt-out instructions, available at the source address of our probes [15]. Over the course of our probing campaigns, we received two opt-out requests with which we immediately complied.

5. RESULTS

We present the following results: *(i)* an analysis of the power of the target sets to yield router addresses in Yarrp6 campaigns; *(ii)* comparisons of Yarrp6 results to other probers performing similar and different trace campaigns; *(iii)* detailed results of high-frequency Yarrp6 campaigns launched from three vantage machines each with 18 different target sets, 54 in total on May 14, 2018 and summarized in Figure 6 and Table 7. The top line in the table is the combined result across all (3) vantages and all campaigns per vantage.

5.1 Topology

In terms of overall discovery, the two best performing target sets are cdn-k32 and TUM. Not only do they produce the largest absolute numbers of interfaces, they continue to reveal new addresses throughout the entire probing duration. As shown in Table 7, they are largely complementary and contribute the two largest shares of interfaces exclusively discovered by single target sets.

Figure 6 lets us compare the fraction of total traces performed for each target set, with with features of the router addresses discovered as a result of those traces. In the small axes on the right of the figure, we isolate just the fraction of exclusive BGP prefixes, and exclusive ASNs for each set, since that is obscured by the shared portion on the main figure.

Lastly, as with the seeds in §3, we used `addr6` to classify the resulting router hop addresses discovered across

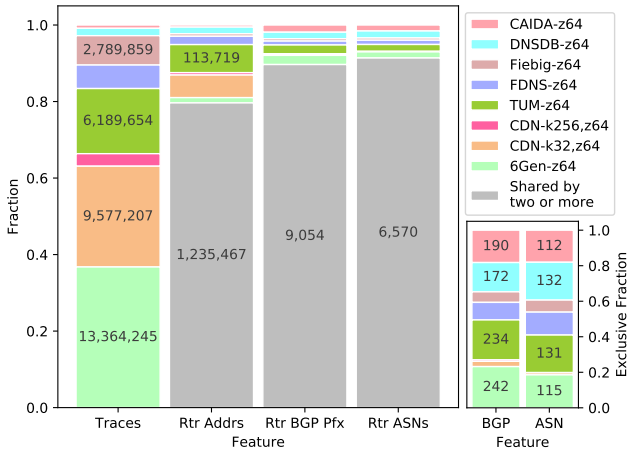

Figure 6: Features of probing results

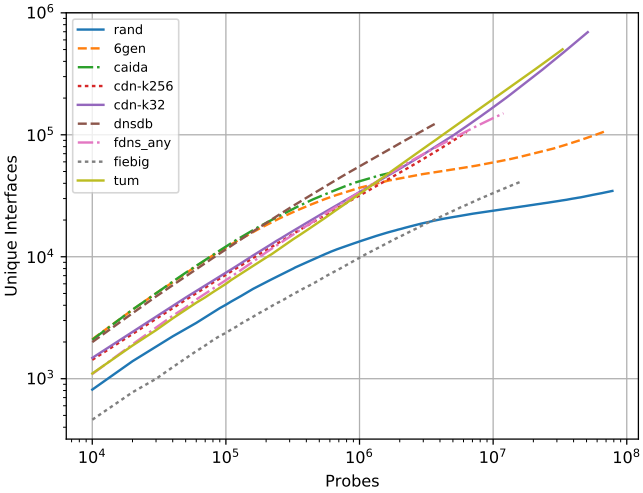

Figure 7: Topological discovery power per z64 aggregated target set vs. probe packets (EU-NET).

all trace campaigns. Surprisingly, we find very many EUI-64 router hop addresses, 651.4k or 45% of all router hop addresses. These are labeled "EUI-64 Hop Addrs" in Table 7, most prominently yielded by the TUM (68% EUI-64 results) and cdn-k32 (39% EUI-64 results) campaigns. Of these EUI-64 router addresses, 59% are from one of just two manufacterers; 99.9% of each of those address are in just two ISP networks, each in different countries. In both cases, WWW content suggests they are Customer Premises Equipment (CPE) routers in ostensibly large, homogenous IPv6 deployments.

It is not a coincidence that these two target sets also have highest overall yield and highest yield of exclusive router hop addresses. This is due, in large part, to elicited ICMPv6 responses from these CPE routers, one target set yielding one manufacturer's routers in one ISP's network and the other finding the other manufacturer's routers in the other ISP's network.

5.2 Target Sets Power

Table 7: Results of aggregate yarrp campaigns run from three vantages, reverse sorted by yield. Rtr Hop Addrs are sources of ICMPv6 Time-Exceeded messages.

Yarrp6 Campaign	Agg	Traces	Target Addrs	Rtr Hop Addrs	Excl Hop Addrs	Rtr BGP Pfxs	Excl Rtr BGP	Rtr ASNs	Excl Rtr ASNs	EUI-64 Hop Addrs	Path Len 95 Perc. (Median)	Reach Target ASN
ALL	both	45.8M	12.6M	1.4M	0	9.9k	0	7.1k	0	651.4k	20 (11)	40%
EU-NET	both	15.0M	12.2M	1.3M	136.0k	9.5k	236	6.9k	110	613.0k	17 (8)	44%
US-EDU-1	both	15.4M	12.6M	1.3M	84.9k	9.4k	75	6.8k	31	602.7k	19 (10)	43%
US-EDU-2	both	15.4M	12.6M	881.4k	20.7k	7.4k	148	5.5k	76	540.6k	21 (15)	33%
cdn k32	z64	9.6M	3.2M	756.6k	91.6k	2.0k	31	1.2k	7	297.2k	18 (12)	52%
tum	z64	6.2M	2.1M	582.4k	113.7k	7.9k	234	6.0k	131	311.2k	19 (12)	63%
cdn k32	z48	1.6M	524.2k	203.7k	16.5k	1.8k	21	1.2k	7	79.8k	19 (12)	70%
fdns	z64	2.2M	746.9k	185.2k	33.8k	6.2k	147	5.0k	80	15.4k	19 (10)	48%
dnsdb	z64	698.6k	233.0k	154.0k	26.8k	7.8k	223	6.0k	132	10.1k	20 (13)	55%
6gen	z64	13.4M	4.5M	126.4k	21.5k	7.1k	242	5.2k	115	24.8k	31 (12)	27%
tum	z48	1.1M	362.7k	118.3k	12.2k	6.6k	172	5.0k	97	11.6k	18 (9)	41%
cdn k256	z64	1.2M	396.7k	116.9k	9.7k	1.2k	9	639	1	28.5k	18 (11)	51%
cdn k256	z48	487.1k	162.4k	89.7k	5.6k	1.1k	11	637	1	19.5k	18 (12)	69%
fdns	z48	673.3k	228.7k	88.5k	8.4k	4.8k	103	4.0k	52	4.2k	18 (6)	29%
dnsdb	z48	281.3k	93.8k	87.9k	10.7k	6.4k	172	5.0k	99	5.5k	21 (12)	49%
6gen	z48	4.3M	1.4M	69.4k	9.6k	6.5k	175	4.9k	103	3.5k	32 (12)	16%
caida	z64	314.7k	105.2k	60.9k	8.5k	6.3k	190	4.8k	112	428	31 (12)	26%
caida	z48	234.3k	78.3k	57.7k	7.9k	6.1k	167	4.7k	99	370	29 (12)	25%
fiebig	z64	2.8M	1.0M	54.2k	10.2k	3.3k	62	2.8k	42	1.3k	17 (5)	24%
fiebig	z48	270.3k	102.2k	22.1k	3.3k	2.7k	45	2.3k	28	177	17 (4)	11%

Central to our study is evaluating trace target strategies to not only maximize topological discovery, but also do so efficiently within an address space too large to be exhaustively probed. In Figure 7, we examine the relationship between each z64 target set's count of unique interfaces discovered via probing from the EU-NET vantage point, and the number of probe packets required.[3] Note that we observe qualitatively similar results from the other vantage points, and choose to focus on the EU-NET results due to space constraints.

The current state-of-the-art strategy, employed by both CAIDA and RIPE for their production IPv6 mapping, of tracing to the `::1` address within routed IPv6 BGP prefixes performs best in the initial stages of the probing, but suffers a noticeable flattening in discovery past 300k packets (note the log-log plot scale). CAIDA's discovery peaks at fewer than 100k interfaces after ≈2M probes as it exhausts the target set. This dichotomy of performing well initially, but falling well short of the absolute number of interfaces discovered via other target sets, illustrates that CAIDA's strategy provides breadth, but lacks the specificity to discover IPv6 subnetting where significant topology exists.

As a second baseline of a BGP-informed strategy, we probe randomly generated IPv6 addresses that are routable. Unsurprisingly, this unguided target selection performs poorly with a precipitous drop in newly discovered interfaces after ∼1M probes. However, random outperforms Fiebig prior to this point, largely due to the high degree of clustering (evident in the DPL of Figure 3). Similarly, the 6gen target set provides a high interface yield at the onset of probing, but flattens past 1M probes. In fact, the shape of the 6gen curve closely mirrors random, but with a fixed positive offset.

In contrast, the overall discovery rate is higher and linear for the TUM and cdn-k32 synthesized target lists, implying that these provide the most power. Even though they provide similar discovery yields, cdn-k32 finds an additional ∼200k interfaces from this vantage.

5.3 Validation

Unfortunately, as with similar Internet-wide measurement studies, comprehensive ground truth is not available. To place our results in context, we therefore consider our discovered IPv6 topologies relative to those available from production IPv6 active traceroute systems, namely CAIDA's Ark [7] and RIPE Atlas [39]. For both, we gather the complete set of traceroute results for May 18, 2018 available from each vantage point. Both Ark and Atlas are global platforms, with vantages in different regions and networks. While Ark had 65 IPv6-capable vantages at the time of writing, Atlas had 4,333.

Within the 24 hour period, Atlas probed 34.3k unique targets and discovered 103.8k unique interfaces, while Ark issued traces to 349k targets which revealed 126.8k interfaces. Notably, while Ark used 6.9M traces, our methodology discovers ≈1.3M interfaces – an order of magnitude more – with only approximately twice the number of traces.

We further compared our results to those of a proprietary prober that regularly performs millions of traces per day. With that prober, the `cdn-k32-z64-fixediid` target set was traced separately on May 3, 2018, i.e. emit-

[3]Equivalently, at our fixed probing rate, this plot shows discovery as a function of time.

ting TTL-limited probes toward active WWW client address space. In contrast to Yarrp6, this prober is stateful, like `traceroute`, and operates by distributing its workload of traces across a set of machines, here, from one physical and topological location to make comparison reasonable. Results show the router hop address yield difference was within 1.1%, and other metrics were similar, suggesting it is plausible that vantage connectivity, alone, could be responsible for the difference.

Lastly, in Table 7, note there is some variation in Yarrp6 results by vantage, despite launching the same campaigns. While EU-NET and US-EDU-1 show similar yield, about 1.3M router hop addresses, US-EDU-2 has lower yield, about 881k, despite having performed just as many traces. Our hypothesis is that this vantage is unusual in that its on-premise path is longer (as seen in Figure 5b and median path length in 7) and thus may warrant a higher TTL value (per §4.2).

6. SUBNET DISCOVERY

Having collected voluminous trace results, we turn our attention to topological inference from the results. We employ two techniques to infer subnet boundaries. The first one is based on path divergence observed in traces from prior work (with IPv4), while the second relies on the ubiquitous delegating of /64 prefixes as the most-specific subnets at the Internet's periphery, thus is IPv6-specific.

Path divergence-based discovery. Inspired by Lee et al. [28], we discover IPv6 subnets based on path divergence detected in the paths traversed in our trace campaigns. However, IPv6 requires different premises. First, our goal is to infer heterogeneous IPv6 prefixes by splitting subnets, starting with known BGP prefixes, into smaller ones based on divergent hops; whereas subnets are coalesced to identify homogeneous IPv4 prefixes in [28]. Next, there is no canonical equivalent of `/24` in IPv6 space due to the freedom afforded network operators by generous address allotments and many transition and feature-based address assignment options.

As in Lee's work, the keys to the technique are twofold. First, traced paths from one or more vantages to two different target addresses are compared to *(a)* identify a *significant* converging subpath (a substring, composed of router hop addresses, that is common to both traced paths) and *(b)* identify a subsequent *significant* diverging subpath. By "significant" we mean we are willing to assume that the divergence, in context of the convergence prior, indicates that the two addresses belong to different subnets. We call the converging subpath by the name "last common subpath" (LCS) and refer to the diverging path tails by the name "divergent suffixes" (DS). The second key to the technique is that, once two addresses are assumed to be in different prefixes, we calculate those two addresses' "discriminating prefix length" (DPL), introduced in §3.4.1. Given that we take them to be in different subnets, we know that the first n bits of each address, where n is the DPL, must also be those of each subnet's base address and the subnet's prefix length (opposite of mask length) must be at least n.

Our implementation, called discoverByPathDiv, classifies sets of IPv6 traced paths as divergent (or not) according to parameters as follows:

- The LCS must have minimum length: $c = 2$.
- The LCS must have C hop(s) having an ASN matching the target's ASN: $C = 1$.
- Missing hop addresses are not allowed in the LCS.
- The last hop's ASN must not match the vantage's ASN: $A = 1$.
- The DS must have minimum length: $s = 1$.
- The DS must have S hop(s) having an ASN matching the target's ASN: $S = 1$.
- No DS can have zero length: $z = 0$.
- The targets' ASNs, for each path pair considered, must match: $T = 1$.

In this way, our implementation (with these numerous parameters) can be made restrictive about the paths it accepts as evidence of significant path divergence and, therefore, conservative in subnet discovery. We tested even more conservative parameter values, e.g. a higher DS minimum length $s = 2$, but path divergences ostensibly due to traffic engineering and load-balancing occurred too near the last hop, as reported also with IPv4 in prior works.

Unfortunately, there are additional complications. For instance, *(a)* IPv6 networks exist that use many ASNs simultaneously, e.g. one originating routes to the BGP prefix(es) covering router addresses and another originating routes for the prefix(es) covering their customer's (target) addresses. To avoid these failing to meet our path and target ASN requirements, we augment the BGP information with collections of "equivalent" ASNs, considering them equal even though they are distinct numbers. Also, *(b)* since it is not necessary for networks to globally advertise their routes to prefixes covering their routers' addresses (since routers only need to talk on LANs or point-to-point links to each other), IPv6 networks also exist that use router addresses not covered in the BGP. To avoid having this violate our path and target ASN requirements, we augment the BGP information with some prefixes that are in Regional Internet Registries but not the global BGP. This is especially important for IPv6 where a small number of very large networks, e.g. Comcast and Charter Spectrum, respectively, present these ASN and IP prefix record keeping challenges.

/64 Discovery. Our second subnet-related topology discovery technique is a simpler one, specific to the

IPv6 Internet which typically has /64 subnets at its edge. This scheme is very common since it is required by popular IPv6 address assignment techniques such as SLAAC (Stateless Address Auto-configuration) and SLAAC with temporary privacy extensions (also known as "privacy addresses") in which every IPv6 host address has an interface identifier (IID) comprising the low 64 bits and a network (subnet) identifier comprising the high 64 bits.

It is often the case that TTL-limited probes to some target address never elicit an ICMP or ICMPv6 response with the target address as its source. This leaves the analyst not knowing whether the resulting path reached the router nearest the target or not, making it hard to make assertions on even simple metrics like the diameter of the Internet (as measured in router hops). To overcome this problem of determine where exactly that last hop is in the topology, we leverage the fact, learned from prior active measurement studies, that many IPv6 routers have the IID value `:0000:0000:0000:0001` (canonically displayed as `::1` with zero compression) in the source address used to generate ICMPv6 error messages such as Time-Exceeded [22], e.g. routers serving as the gateway for hosts having address in the subnet for that LAN. Certainly not all IPv6 routers do this, but it is common and is not unlike the practice with IPv4 of, for example, using `192.168.0.1` as the router gateway address for the `192.168.0.0/24` subnet. When we see a last hop ending in *::1* that has the high 64-bits matching the target address, we assume that the probe elicited a response from the router for the target's LAN, and thus completed. This is a valuable inference in at least two ways: *(a)* it allows us to assume this trace reached a unique subnet and thus the target address must be in a different subnet than another target address that, likewise, has a last hop it its own /64 covering prefix, thereby enabling divergence-based discovery; *(b)* it can help us infer reachability, access control, and firewalling policies and limit results in active measurement campaigns, e.g. to assess vulnerabilities or to discover topological characteristics.

We added this second technique to discoverByPathDiv and call it the "Identity Association (IA) Hack" because it can be leveraged to reverse-engineer the IP address identity (prefix) delegated to a customer by an ISP. This is is an important capability for privacy-minded Internet operation if we wish to guarantee some level of anonymity in IP addresses [36]; we are pursuing this as future work.

Candidate Subnet Results. We refer to our results as "candidates" because our method determines a lower bound on a subnet's prefix length. This bound is limited by the highest DPL of a target address ostensibly within the subnet and another ostensible without, i.e. where the traces show paths to those targets diverged. Thus,

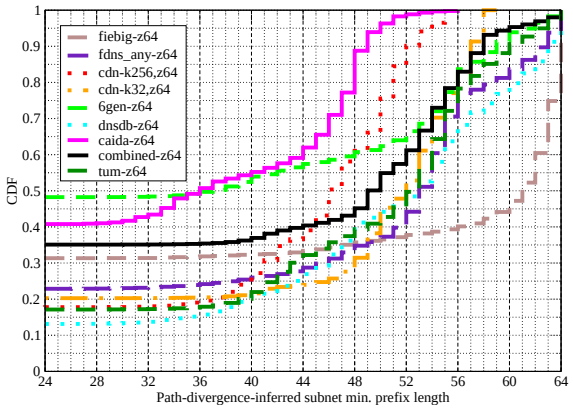

(a) Dist. of min. subnet prefix lengths

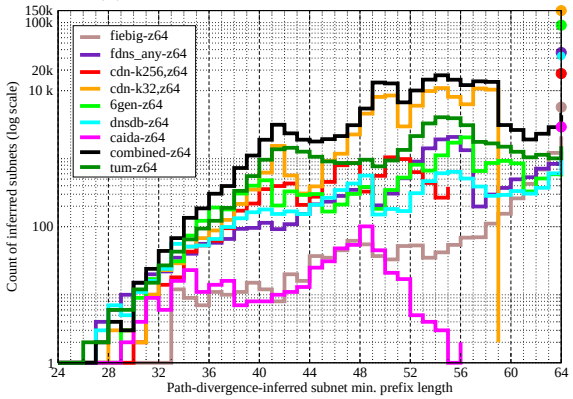

(b) Counts of subnets by prefix length

Figure 8: Subnets inferred by path divergence

a candidate subnet length means that we've discovered a subnet having a prefix length of *at least* that reported.

Examining the combination of all 45.8M traces for path divergences, we find discovered 172,497 candidate subnets, covered by 1,726 BGP prefixes having 1,013 origin ASNs. Figure 8a plots the CDF of those subnets for each target set. This figure shows that target sets power to discover candidate subnets is largely governed by their respective addresses' DPLs plotted in Figure 3a. Also note that, although we see improved *potential* power of the targets sets in combination (Figure 3b), that potential is not evident here: the CDFs do not shift right This unrealized may be due to active measurement difficulties, e.g. missing hops on traced paths and our conservative approach which does not allow missing hops on the common subpath before divergence.

In Figure 8b, we plot counts of discovered subnets by prefix length per target set and combined. Note there are a few prominences suggesting popular prefix lengths (subnet sizes). Also note that, while some target sets help to discover only subnets less than a particular length, e.g. 59 (`cdn-k32`) or 55 (`cdn-k256`), others can help to discover more specific subnets because they contain unanonymized (public) /64 prefixes, e.g. from the DNS. The dots plotted directly above 64 on the horizontal axis

in Figure 8b are the counts times the last hop address was covered by the same /64 prefix as the target address, i.e. the IA Hack. (Combined these total to 1,284,891.)

Subnet Validation. To evaluate these results, we use as set of ground truth data consisting of a set of 12,447 interior prefixes of major US ISP networks (109 BGP prefixes advertised by 30 origin ASNs) and their respective city-level geographical locations and assume they are also topologically heterogeneous, i.e. in different subnets such that our our method should be able to ascertain, if it is given sufficient traces to target addresses in and near those subnets.

We find, that we've performed 386,579 traces from each vantage to target addresses covered by 5,839 (47%) of the subnets in truth data. Of those, our algorithm discovered 109 subnets exactly as in the truth data, i.e. having the same base addresses prefix lengths: 107 /40 prefixes and 2 /64 prefixes. However, because these ground truth subnets are intermediate (in between advertised BGP prefixes and LAN subnets) or "distribution" subnets, we shouldn't expect many exact matches as our method may have discovered more-specific subnets. Indeed we find that we've discovered more specific candidates within 3,871 (66%) of those ground truth prefixes.

To deal with this complication, we re-run our algorithm on a subset of traces selected by stratified sampling, i.e. we choose only one trace to one target address in each ground truth subnet. This intentionally reduces the fidelity of our technique by lowering the target addresses' DPLs, thus limiting discovery to subnets no more-specific than those in the truth data. With this sampled subset of traces our algorithm yields 914 candidate subnets (18%), 395 (43%) of which are exactly as in the truth data. Of the non-matching results, 52% are of prefix length short by one bit and 20% are short by two. Improving this prefix length approximation by lower bound necessitates additional traces to targets with higher DPL. As such, we merely claim these discovered subnet results are plausible based on modest coincidence with ground truth and that stratified sampling is a possible way the technique can be tuned to discover hierarchical subnets.

7. DISCUSSION AND FUTURE WORK

In this work, we seek to advance the state-of-the-art in Internet-wide IPv6 active topology mapping. We collect and synthesize IPv6 targets from a number of sources using a three-step process. Next, to facilitate large-scale IPv6 topology mapping, we emit traceroutes from three vantage points to the targets using a modified version of Yarrp. Along the way, we investigate the use of various target selection methods and parameters (*e.g.*, maximum TTL, probing speed, etc.) that elicit the most IPv6 topological information. Our investigations provide breadth across networks, depth to discover subnetting, and speed. More specifically, we discover over 1.3M IPv6 router interfaces, which is an order of magnitude more compared to the state-of-the-art mapping systems.

7.1 Security

Our results led us to consider security concerns specific to IPv6 topology mapping. Due in part to the address length, IPv6 router addresses can contain sensitive information that makes the active IPv6 address space easier to scan or probe, and likely more vulnerable to malicious exploits [20]. For example, our probe campaigns generated ICMPv6 time exceeded responses from many sources with EUI-64 addresses. These IIDs ostensibly embed Ethernet addresses, exposing the manufacturer and model of a router [33]. Likewise, we received Time Exceeded messages sourced from many router addresses, often with IID of `::1`, covered by the same /64 prefix as the target address. The community should more carefully consider the implications of this address /64 co-location as the source address, alone, can disclose details that users may prefer to remain private.

Therefore, we chose to release two IPv6 topology datasets with different restrictions. The publicly available topology, available at [5], removes hops containing EUI-64 addresses, as well as those addresses covered by the same /64 prefix as a target address. The complete topology will be available to researchers at [14] with restricted distribution. However, we note that our methodology is reproducible using publicly-available seed datasets and freely-available probe utilities. The resulting addresses and subnets discovered or inferred likely extend the attack surface already provided by the hitlists to routing infrastructure.

7.2 Future Work

Based on these encouraging results, we plan to leverage our methodology across a large number of vantages and time to provide even greater scope and coverage. Further, we plan to perform alias resolution, e.g. [30], to produce router-level topologies and facilitate comparative graph analyses between IPv4 and IPv6.

Finally, our subnet discovery results show that it is sometimes feasible to remotely determine likely IPv6 prefix assigned to a single user or subscriber In DHCPv6 prefix delegation this is referred to as Identity Association (IA), and prefix lengths can vary according to the services offered and hints offered by a router to which a prefix is delegated, e.g. on the customer premises. We plan to run additional measurement campaigns to comprehensively assess this capability, with the hope that it might inform IP address anonymization by aggregation, to provide a known level of client privacy.

8. REFERENCES

[1] University of Oregon RouteViews, 2016. http://www.routeviews.org.

[2] P. Alvarez, F. Oprea, and J. Rula. Rate-limiting of ipv6 traceroutes is widespread: measurements and mitigations., 2017. https://www.ietf.org/proceedings/99/slides/slides-99-maprg-rate-limiting-of-ipv6-traceroutes-is-widespread-measurements-and-mitigations-02.pdf.

[3] B. Augustin, X. Cuvellier, B. Orgogozo, F. Viger, T. Friedman, M. Latapy, C. Magnien, and R. Teixeira. Avoiding traceroute anomalies with Paris traceroute. In *Proceedings of ACM IMC*, 2006.

[4] R. Beverly. Yarrp'ing the Internet: Randomized High-Speed Active Topology Discovery. In *Proceedings of ACM IMC*, Nov. 2016.

[5] R. Beverly and J. Rohrer. Yarrp6 Beholder Datasets, 2018. https://www.cmand.org/yarrp/ipv6/.

[6] CAIDA. The CAIDA UCSD IPv4 Routed /24 Topology Dataset, 2016. http://www.caida.org/data/active/ipv4_routed_24_topology_dataset.xml.

[7] CAIDA. The CAIDA UCSD IPv6 Topology Dataset, 2018. http://www.caida.org/data/active/ipv6_allpref_topology_dataset.xml.

[8] M. P. Collins, T. J. Shimeall, S. Faber, J. Janies, R. Weaver, M. De Shon, and J. Kadane. Using uncleanliness to predict future botnet addresses. In *Proceedings of the 7th ACM SIGCOMM conference on Internet measurement*, 2007.

[9] A. Conta, S. Deering, and M. Gupta. Internet Control Message Protocol (ICMPv6) for the Internet Protocol Version 6 (IPv6) Specification. RFC 4443, Mar. 2006.

[10] J. Czyz, M. Allman, J. Zhang, S. Iekel-Johnson, E. Osterweil, and M. Bailey. Measuring IPv6 Adoption. In *ACM SIGCOMM*, Aug. 2014.

[11] J. Czyz, M. Luckie, M. Allman, and M. Bailey. Don't Forget to Lock the Back Door! A Characterization of IPv6 Network Security Policy. In *Network and Distributed Systems Security (NDSS)*, 2016.

[12] A. Dainotti, K. Benson, A. King, M. Kallitsis, E. Glatz, X. Dimitropoulos, et al. Estimating Internet Address Space Usage through Passive Measurements. *ACM SIGCOMM CCR*, 2013.

[13] A. Dhamdhere, M. Luckie, B. Huffaker, k. claffy, A. Elmokashfi, and E. Aben. Measuring the Deployment of IPv6: Topology, Routing and Performance. In *Internet Measurement Conference (IMC)*, Nov 2012.

[14] DHS. IMPACT Cyber Trust, 2018. https://www.impactcybertrust.org/.

[15] Z. Durumeric, E. Wustrow, and J. A. Halderman. Zmap: Fast internet-wide scanning and its security applications. In *USENIX Security*, 2013.

[16] T. Fiebig, K. Borgolte, S. Hao, C. Kruegel, and G. Vigna. Something From Nothing (There): Collecting Global IPv6 Datasets From DNS. In *Proceedings of the 18th Passive and Active Measurement Conference*, Mar. 2017.

[17] P. Foremski, D. Plonka, and A. Berger. Entropy/ip: Uncovering structure in ipv6 addresses. In *Proceedings of ACM IMC*, 2016.

[18] O. Gasser, Q. Scheitle, S. Gebhard, and G. Carle. Scanning the ipv6 internet: Towards a comprehensive hitlist. In *Workshop on Traffic Monitoring and Analysis*, Apr. 2016.

[19] E. W. Gaston. High-frequency mapping of the IPv6 Internet using Yarrp. Master's thesis, Naval Postgraduate School, 2017. http://hdl.handle.net/10945/52982.

[20] F. Gont and T. Chown. Network Reconnaissance in IPv6 Networks. RFC 7707 (Informational), Mar. 2016.

[21] Google. Ipv6 adoption statistics, 2018. https://www.google.com/intl/en/ipv6/statistics.html.

[22] M. D. Gray. Discovery of IPv6 router interface addresses via heuristic methods. Master's thesis, Naval Postgraduate School, 2015. http://hdl.handle.net/10945/47265.

[23] R. Hinden and S. Deering. IP Version 6 Addressing Architecture. RFC 4291 (Draft Standard), Feb. 2006.

[24] G. Huston. Bgp routing table analysis, 2018. https://bgp.potaroo.net/index-v6.html.

[25] k. claffy, Y. Hyun, K. Keys, and M. Fomenkov. Internet mapping: from art to science. In *IEEE Cybersecurity Applications for Homeland Security*, Mar. 2009.

[26] A. J. Kalafut, C. A. Shue, and M. Gupta. Malicious hubs: detecting abnormally malicious autonomous systems. In *INFOCOM*, 2010.

[27] E. Kohler, J. Li, V. Paxson, and S. Shenker. Observed Structure of Addresses in IP Traffic. In *Internet Measurement Workshop*, pages 253–266, 2002.

[28] Y. Lee and N. Spring. Identifying and aggregating homogeneous ipv4/24 blocks with hobbit. In *Proceedings of the 2016 Internet Measurement Conference*, 2016.

[29] M. Luckie. Scamper: a scalable and extensible packet prober for active measurement of the Internet. In *IMC*, Nov. 2010.

[30] M. Luckie, R. Beverly, W. Brinkmeyer, and kc claffy. Speedtrap: Internet-Scale IPv6 Alias Resolution. In *Proceedings of the ACM SIGCOMM Internet Measurement Conference (IMC)*, 2013.

[31] M. Luckie, Y. Hyun, and B. Huffaker. Traceroute Probe Method and Forward IP Path Inference. In *Internet Measurement Conference (IMC)*, Oct 2008.

[32] D. Malone. Observations of IPv6 Addresses. In *Passive and Active Network Measurement*, 2008.

[33] J. Martin, E. C. Rye, and R. Beverly. Decomposition of MAC Address Structure for Granular Device Inference. In *Proceedings of the 32nd Annual Computer Security Applications Conference (ACSAC)*, Dec. 2016.

[34] A. Murdock, F. Li, P. Bramsen, Z. Durumeric, and V. Paxson. Target generation for internet-wide ipv6 scanning. In *Proceedings of ACM IMC*, 2017.

[35] D. Plonka and A. Berger. Temporal and spatial classification of active ipv6 addresses. In *Proceedings of ACM IMC*, 2015.

[36] D. Plonka and A. W. Berger. kIP: a Measured Approach to IPv6 Address Anonymization. *CoRR*, abs/1707.03900, 2017.

[37] D. Plonka and K. Rose. A continuing study of the active www client address space, 2018. https://datatracker.ietf.org/meeting/100/materials/slides-100-maprg-a-continuing-study-of-the-active-ipv6-www-client-address-space-kyle-rose/.

[38] Rapid7. Forward dns datasets, 2018. https://scans.io/study/sonar.fdns_v2.

[39] RIPE NCC. RIPE Atlas, 2018. https://atlas.ripe.net/.

[40] J. P. Rohrer, B. LaFever, and R. Beverly. Empirical Study of Router IPv6 Interface Address Distributions. *IEEE Internet Computing*, Aug. 2016.

[41] F. Security. Passive dns project, 2018. https://www.farsightsecurity.com/technical/passive-dns/.

[42] SI6 Networks. SI6 Networks' IPv6 Toolkit. https://github.com/fgont/ipv6toolkit, 2016.

[43] N. Spring, R. Mahajan, and D. Wetherall. Measuring ISP topologies with Rocketfuel. *ACM SIGCOMM Computer Communication Review*, 32(4), 2002.

[44] M. Syamkumar, R. Durairajan, and P. Barford. Bigfoot: A geo-based visualization methodology for detecting bgp threats. In *Visualization for Cyber Security (VizSec)*, 2016.

[45] J. Ullrich, P. Kieseberg, K. Krombholz, and E. Weippl. On reconnaissance with ipv6: a pattern-based scanning approach. In *Availability, Reliability and Security (ARES)*, 2015.

[46] Z. Zhang, Y. Zhang, Y. C. Hu, Z. M. Mao, and R. Bush. Ispy: detecting ip prefix hijacking on my own. In *ACM SIGCOMM Computer Communication Review*, 2008.